Elemental Quantification in three dimensions using electron beam microanalysis

2246197K

University of Glasgow, School of Physics & Astronomy

The aim of this project to was to develop a method to analyse and align a stack of 2D elemental maps to enable quantifed compositional analysis in three dimensions.

Abstract. The elemental quantification of a metal alloy sample is a simple process when using an advanced analysis software such as Bruker Espirit. However even these programs fail to incorporate key aspects of sample analysis such as drift correction and specific regional selection, which if allowed for enable a more in-depth investigation of the material. Energy dispersive x-ray spectroscopy (EDS) is a technique that produces a two-dimensional map of the distribution of chemical elements on the surface of a sample. Recent developments now facilitate the serial acquisition of a stack of such maps, collected as successive slices are removed from the sample surface; these can then be processed post-acquisition to produce a three-dimensional chemical map. The aim of this project was to improve 3d chemical mapping by (i) implementing algorithms to reduce noise and remove background signal from individual spectra and (ii) correct for sample drift effects. This method was successful in removing the noise components and retaining the important data and allowed quantification via the Cliff-Lorimer method to be performed. Comparison with Bruker quantification methods found the atomic percentage results all agreed within 3% (Table 2) suggesting its accuracy was good in relation to comparable software. While the discrepancies in values were mostly due to how accurately each method can isolate and sum the spectra changes in quantification input specifications would allow for an even closer accuracy with Bruker.

1. Background

To first understand how to quantify the elemental composition from an Electron Dispersive X-ray spectroscopy (EDS) spectrum for a thermoelectric sample it is important to investigate what a thermoelectric is and hence what you are likely to see. A thermoelectric device is a metal-alloy that works by converting heat gradients into electrical energy. The materials must have high electrical conductivity and low thermal conductivity to give the best thermoelectric response. Low thermal conductivity ensures that when one side is heated the other will stay cool and maintain a temperature gradient, hence generating a larger voltage. At the intersection between two different kinds of wires the Seebeck effect transforms heat into electricity: when the junction is heated electron energy levels are shifted differently in the separate metals, creating a potential difference between the wires, which in turn creates an electrical flow through the wires. If the wires are connected in a circuit a current is produced [1].

A Scanning Electron Microscope (SEM) was used to image the samples which moves over the surface scanning the face with a focused beam of electrons. The electrons interact with the atoms in the

sample emitting signals that allow the operator to determine information about the chemical makeup and facial topography of the sample [2]. The electron beam is scanned in a raster scan pattern, where the beam scans left to right along one line and then returns to the left side to begin the next line, similar to the reading of a book. When the primary electron beam interacts with the sample, random scattering and absorption cause the electrons to lose energy within a pear-shaped volume of the sample known as the interaction volume. The dimensions of the interaction volume depend on the specimen density, the electrons energy at the surface and the atomic number of the specimen. The energy exchange between the electron beam and the sample results in the emission of electromagnetic radiation, the reflection of high-energy electrons by elastic scattering and the emission of secondary electrons by inelastic scattering, each of which can be detected by specialised detectors [3].

The position of the beam is combined with the intensity of the detected signal to produce an image. The number of secondary electrons excited by the electron beam are detected by a secondary detector, this along with the signal intensity, depend primarily on the specimen topography. Backscattered electrons are reflected back out of the specimen interaction volume by elastic scattering with specimen atoms and consist of high-energy electrons which originated in the electron beam. Heavy elements backscatter more strongly than light elements and so appear brighter in the image, hence the technique can be used to distinguish variation between areas of contrasting chemical composition [3].

Whilst the SEM image gives the shape and visual structure, Energy-dispersive x-ray spectroscopy (EDS) provides information about the atomic components [4]. A high energy electron beam is used to analyse the sample and relies on the fact that each element has a varying atomic arrangement, resulting in different energy radiation being released depending on the specific atomic energy levels of the elements in the sample. At rest atoms within the sample contain ground state electrons in discrete energy levels. When the beam hits the sample, electrons in an inner shell may become excited and get ejected from the atom creating an electron hole. This empty hole is filled by one of the outer electrons and the difference between the energy levels is released as an x-ray. The number and energy of x-rays is measured by an energy-dispersive spectrometer generating a unique spectrum for each element at the x-ray emission lines of each of the components that are contained in the sample.

During the collection of the data, drift can occur between measurements due a variety of reasons. If the sample increases in temperature during the measurement process then thermal expansion can lead to drift as measurements are being taken with such small differences. Mechanical vibrations, if significant enough, can also lead to a slight drift in the image or if the sample is not sufficiently fixed in place the sample itself may move between measurements. It is possible for the electron beam to drift which can occur by specimen charging, this is the build-up of negative charge on the surface of a sample that is being irradiated with an electron beam [5]. For electron microscopy it is vital to have good electrical conductivity, and if this is not satisfied the beam can drift away from the sample if it is negatively charged, leading to measurement of the wrong area of the sample.

In this project, I dealt with the issue of drift correction by using aspects of an open source Python library called Hyperspy [6], which specialises in EDS and EELS data analysis. Alongside this I implemented my own code and adjustments to the pre-existing code to create an algorithm that would identify shifts between measurements and applying this to both the SEM and EDS data. To this corrected dataset a noise correction technique called non-negative matrix factorisation (NMF) was applied before finally preparing the required metadata for the sample and applying a Cliff-Lorimer quantification method.

2. Experimental Methods

2.1. Preparation and Alignment

To examine the sample the whole dataset was loaded into the Python program which consisted of a 2D SEM image, a 2D EDS image with an individual spectrum contain in each pixel of the image, and an Electron Backscatter Diffraction (EBSD) component that contained information about the crystallographic structure. EBSD is not required for the image correction and is the largest file size in the dataset so the SEM and EDS data were extracted to be explored separately. Before determining any compositional characteristics of the material the first step is to correct the sample for drift, and if any has occurred, applying this correction to both the SEM and EDS data.

Before finding the shifts that have resulted from the image drift, as described below, I use the Hyperspy algorithm to find these shifts, but first pre-process the data to improve the accuracy of the shift measurements. The first pre-processing method that can be used is a Sobel filter which improves the definition of the edges of the image, enabling a more accurate comparison between images. Secondly a median filter can be used to reduce noise although this also creates a blurring effect on the image as it uses an average of neighbouring pixels method. Finally, a Hanning filter can be used which performs a smoothing fit to a bell curve; note it was found that not using a Hanning filter produced no shift vectors. Not using a Sobel filter produced the smallest shifts, but when viewing the final alignment it was clear that the shifts were not large enough to adequately align the whole stack, and so it was necessary to include this filter. Not using a median filter produced the largest shifts. It was therefore decided that use of the Sobel and Hanning filters produced the magnitude of shift that was needed. After the filters were applied, cross-correlation was used to calculate the shift vectors for all image pairs [7].

The Hyperspy algorithm finds an initial shift vector for every slice in reference to the first slice in the stack. This is done by identifying areas of pixels that form the same structures between images. Hence it is vital to have points of reference between the images with more points of reference allowing for a more accurate result. From the SEM images a single layer from the top face is milled between each scan but the main body of the alloy remains constant, and so this will act as a good reference (Fig 2). Furthermore, the sample is held into place by a platinum stand which will remain fixed between measurements and will only change position if it is subject to drift, so it will be another good reference point. It is vital that both the full body and the clamp are included when determining the shift vectors. Statistical analysis is performed next to exclude incorrect shift vectors and allow the algorithm to select an optimum reference image. In this step incorrect shift vectors are excluded if the user has set a maximum absolute value limit for the shifts. For every image shifts are calculated in relation to the other images and a quality measure of this value is determined. The image with the highest quality value was chosen as the new basis for cross-correlation to find new shift vectors which were then applied to the SEM image [7]. To determine whether an accurate shift result is found out-with the code, comparisons were made between an aligned and unaligned stack of the SEM data to ensure the shifts had been applied correctly.

Before the EDS data is examined in more detail the previously identified shift is now performed on the respective data. The EDS data is only taken for the milled face of the sample whereas an SEM image is taken for the whole sample and background platform. The EDS file has the same dimensions as the SEM file but since only the milled face contains EDS data (Fig 2**,** face inside red section) there is a large section of the dataset that contains no information. Therefore an interactive rectangular crop is used which allows this data to be removed to speed up the data processing and reduce the size of the data that needs to be stored. The shift is performed using a “roll” technique where the data is shifted horizontally and vertically, where data that is shifted off the top (or side) is then replaced on the bottom (or opposite side), so no data is lost. For the recreation of a 3D sample any data that does not overlap with all other slices is not useful and so a new region of interest is selected using the

maximum shift vectors in all directions to exclude any data that cannot be used. Additionally, if there is any significant noise at the edges of the spectrum this was removed.

2.2. Noise reduction

When first evaluating the EDS data there is a need to perform noise reduction techniques to remove irrelevant data that obscures the desired information in order to improve the accuracy of the results. In an EDS spectrum this noise can include false peaks that appear due to x-rays being produced from components of the microscope, or random noise which is produced when electrons are randomly excited producing x-rays that are not expected [8]. To identify the components of the data that contain signal and noise, principal component analysis (PCA) is performed to help determine the dimensionality of the data. PCA works by reducing a large set of variables to a smaller set that still contains most of the information in the larger set but with the aim of excluding any noise components. This is done by transforming a number of correlated variables into a smaller number of uncorrelated variables called principal components. The data are split into these variables where the first principal component contains the direction with the largest variance. For example, if you have a scatter plot (Fig 1) and draw a straight line across it, a line which has the largest distance between the two end points it spans and the shortest perpendicular distance to points in relation to this line will have the greatest variance. This line will be a combination of the two variables on the x and y axis and will be the first principal component as shown in fig 1, with the second principal component orthogonal to the original PCA component ensuring the same factors apply. When viewing PCA 1 this gives all the components projected onto the single PCA 1 axis and will contain most of the relevant data. However, recreating the original dataset it requires a combination of PCA 1 and 2 which then allows you to determine the original position of the points. To determine the components to keep, a scree plot of variance components can be plotted against the proportion of total variance (with total being 1). Additionally, each separate variance component can be plotted and viewed visually and for higher dimension datasets there are more PCA components [9]. This enables us to tell which components are real signals and which are just noise.

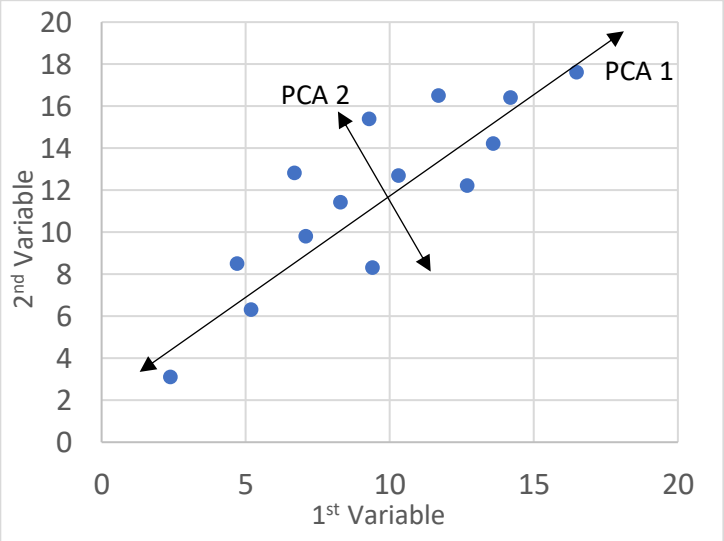

Figure 1. PCA principles in a 2D example dataset

PCA in this application is used to determine the number of components to subsequently pass through a non-negative matrix factorisation (NMF) method. NMF is similar to PCA, in the way it splits up the data into multiple matrices (NMF eigenvectors that multiply together to give the original dataset), however in NMF all values are forced to be positive [10]. This is extremely beneficial for EDS data as other PCA/ICA methods may produce negative values which do not signify real properties on an EDS spectrum. The EDS spectrum is quantified by summing the spectra over the width of the peak and shifts

in the energy of the peak that produce these negative values in PCA will give false results. To noise reduce the data, NMF is applied to the spectrum using the information gained about the dimensionality of the data from PCA. The components of NMF can be checked and those eigenvectors that are attributed to noise are removed from the data.

2.3. Quantification

Once noise reduction has been performed the EDS data must then be processed by adding the required metadata so that it can be analysed using the Cliff-Lorimer quantification method [11]. The elements present in the sample must be known although it is not necessary to know the proportion of each beforehand. The elements are added to the EDS metadata and will be used for quantification, by using the beam energy of the microscope to add the possible x-ray lines to the metadata. To better fit the spectrum, it is important to remove background noise that arises from the Bremsstrahlung (or braking radiation) which is produced when a charged particle is decelerated by another charged particle, i.e. the change in kinetic energy being transformed into radiation producing the characteristic background curve. To remove this background effect windows either side of each peak are set in sections where there is no peak, and when quantification is performed this background will be subtracted to give accurate values. For the preparation of quantification integration windows are selected, within which the intensity of counts are summed to find the amounts of each element. It is important to select a wide enough region so that all the counts are measured but not so wide that it overlaps a separate elements energy peak.

The Cliff-Lorimer method uses the equation,

$$\frac{C_A}{C_B} = k_{AB} \cdot \frac{I_A}{I_B}$$

Where C_A/C_B is the concentration ratio of element A to element B. k_{AB} is the ratio of the k factors for A and B which relate the compositions of the constituent elements to the measured characteristic x-ray intensities above background. The k factors are unique to each element and the electron microscope setup, and are determined by ionisation cross-sections and fluorescent yields. They allow for the accurate determination of percentages and atomic weights of measured objects. I_A and I_B are the measured intensities of the elements.

3. Results and Discussion

3.1. Raw SEM

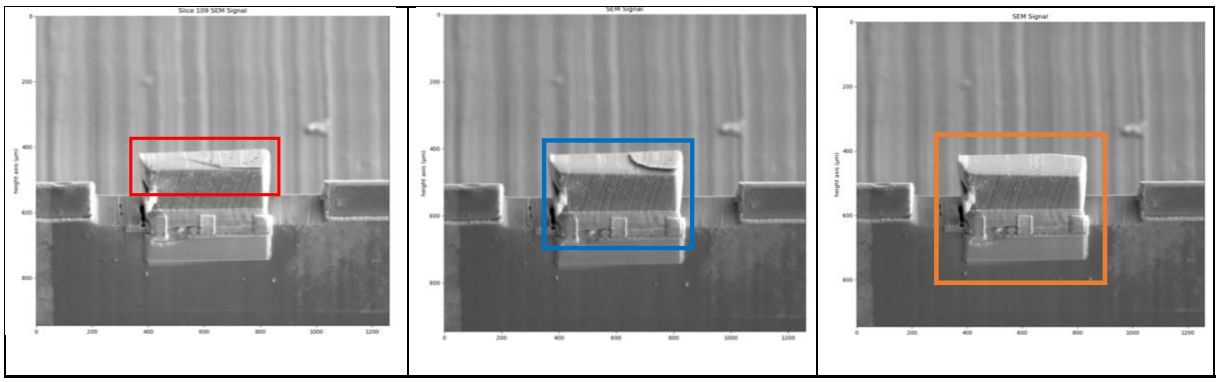

Figure 2. Areas selected for cross referencing analysis

When determining shift vectors, it is important to keep a high number of points of reference for the alignment algorithm to give more accurate results. It was therefore vital to include a large enough area for analysis but not so large that computation times become too extreme, and it was found that computational times over 30 minutes would not result in dramatically better results. The algorithm looked for sections of pixels that were arranged in the same formations between images, and so the more similar the images were, the better the results. Only the face (central section in red box) changed as can be seen between the images (Fig 2), and so it was a good selection for the outcome needed. The end sloped face of the sample and a section of the main body were the only areas that were evaluated for EDS and EBSD data. Inside the sloped section there were some dark structures on the face likely corresponding to a ledge on the surface. Through later slices the ledge moved and became more prominent, so it was interesting to see how this caused any artefacts or changes in results. It was discovered that the area along the ledge showed a deficiency in titanium but an increase in nickel and tin (Fig 9). It was useful to compare the use of filters to determine if they were all required. Whilst analysing the full image would give the most reference points, on a more powerful computer it was estimated this would take 80 minutes for a stack of 90 slices. Taking a smaller area (selected in blue) whilst retaining the whole alloy and the holder, which provided the main point of reference between images, allowed for a good determination of shift vectors and took a more practical 11-12 minutes to perform. Increasing the area of cross-referencing affected the maximum and average shift vectors dramatically so it is extremely important to keep as large as possible.

Table 1. Comparison of max shift vectors (units of pixels)

Size of Region	**Max shift up**	**Max shift down**	**Max shift left**	**Max shift right**	**Average up/down**	**Average left/right**
Small (red)	4.36	-7.36	-9	0	-1.26	-3.89
Medium (blue)	5.23	-15.7	-5.83	0	-6.57	-2.23
Large (orange)	5.3	-21.3	-2.13	0	-7.83	-1.86
Medium (blue*)	5.3	-16.3	-5.7	0	-6.57	-2.23

*No median filter used

Table 1 shows the maximum shift vectors measured using the method described and demonstrates that large areas for cross-correlation give larger shifts. However as the area increased the magnitude increase of the shift was smaller. When looking at the need for filters to prepare the image for the same size area, removing the median filter produced very similar shifts, and for the medium size area the computation time was reduced by 4 minutes, only taking 8 minutes to perform. The median filter's purpose is to reduce noise but it also has a side effect of blurring the image, which would not benefit the determination of shifts, so this filter was not used. Table 1 assists in determining the need for the filters along with finding the limits on the size of region selected and how this affects shift values. To determine the quality of these shifts the individual shift vectors and resulting image alignment are necessary and will be inspected next. The other two filters were found to be necessary to produce any shift and so were retained.

3.2. Alignment

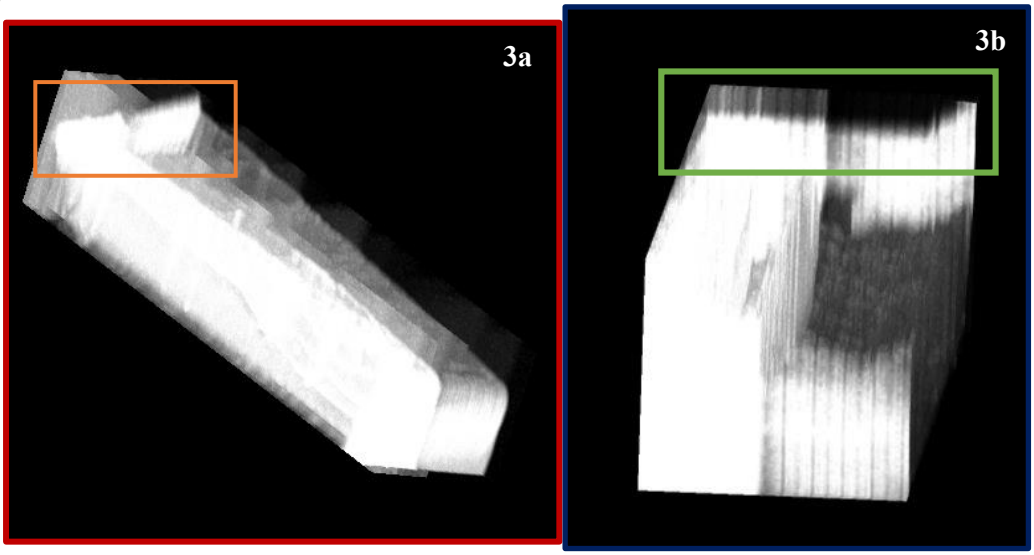

Figure 3. Unaligned (3a) and Aligned (3b) SEM stacks

To evaluate the quality of alignment it is possible to view the shift vectors and ensure that they are realistic in relation to the size of the image. A shift half the size of the image is not likely considering the sample is not moved between measurements, and it is therefore only outside factors on the sample during measurement that will produce a shift. Plotting a 3D image (Fig 3) of an unaligned stack (red) by looking at the end of the stack (in orange) the slice slopes downwards from right to left when it should be a flat line, and so there is a need for some alignment because the stack has been shifted up slightly between each successive measurement. Alternatively flicking through individual SEM diagrams the position of constant points between images clearly moves and so alignment is necessary. From an aligned stack (blue) looking at the same end (green), the top of the sample is now aligned so that consecutive slices are placed on top of one another.

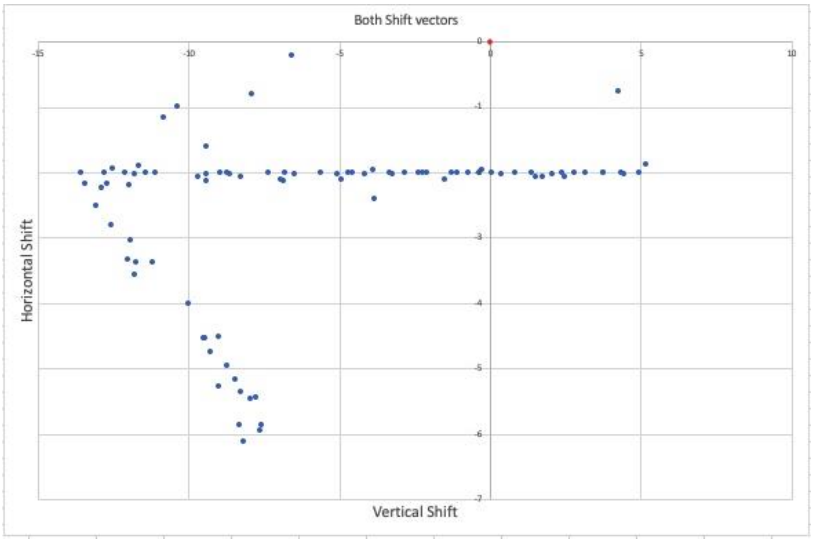

Figure 3c. Shift vectors applied to SEM in Fig 3 (red point shows reference slice)

As seen in Figure 3c, there is a correlation between the vectors since a large number show a similar horizontal shift vector with increasing (magnitude) of vertical shift, which is constant with the drift between images that was expected. If a wrong reference slice had been chosen or the cause of the shifts were random then there would be little correlation and shifts would be random. There is a change once the vectors reach a maximum negative vertical shift where their horizontal shift increases dramatically. From inspection of individual faces there is not a clear major visible change that would cause this however changes in measurement conditions may have caused the drift to change direction.

3.3. Energy dispersive x-ray spectrometry (EDS)

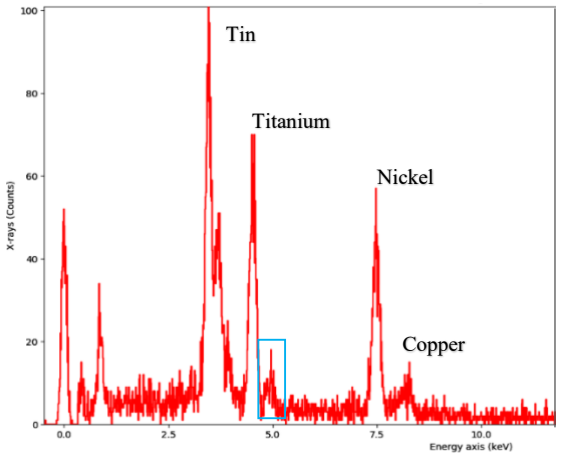

Figure 4a. Raw EDS spectrum

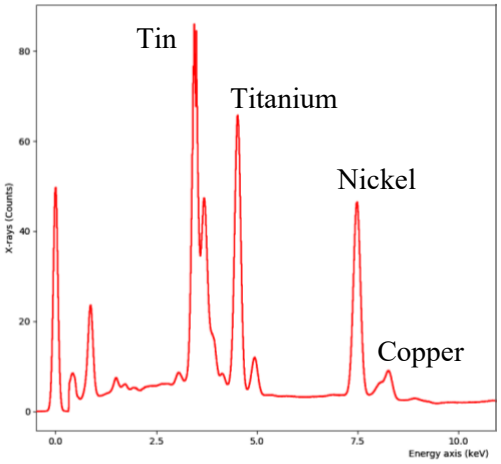

Figure 4b. Noise reduced EDS spectrum

Once shifts were determined from SEM data they were applied to the EDS and the new data was cropped via a code which I wrote to only include overlapping sections that contained data. This is necessary because if one slice is shifted 5 pixels right and a separate slice 5 pixels left then there is now a horizontal section of 10 pixels in total that only contains data for one slice but not the other. As we are viewing this in 3D it is not useful to keep data that cannot be shown through the whole stack so it is removed. It is possible to perform quantification on raw EDS data but the amount of noise in the image makes it more difficult to determine an accurate background value to use for subtraction when calculating results, and so there will be a greater error in any final values. Any small peaks will be obscured in the data if the noise exceeds or equals the value of the peak and for accurate quantification it is vital to take into account all measured useful counts. Removing noise allows the spectrum to be examined in more detail identifying any irregularities to be studied and ensures that the spectrum matches what is expected. This means that no counts or small peaks are viewed that are not expected, suggesting that the instrument is either measuring an element from another part of the detector or there is some error in the equipment resulting in a signal that is not real. In Figure 4, the area in blue could have been considered just noise and not a useful peak since it does not correspond to a major emission line, however it was determined (through analysis on the Bruker software) to be a component of the titanium peak and so was included when determining the titanium component.

3.4. Principal Component Analysis (PCA)

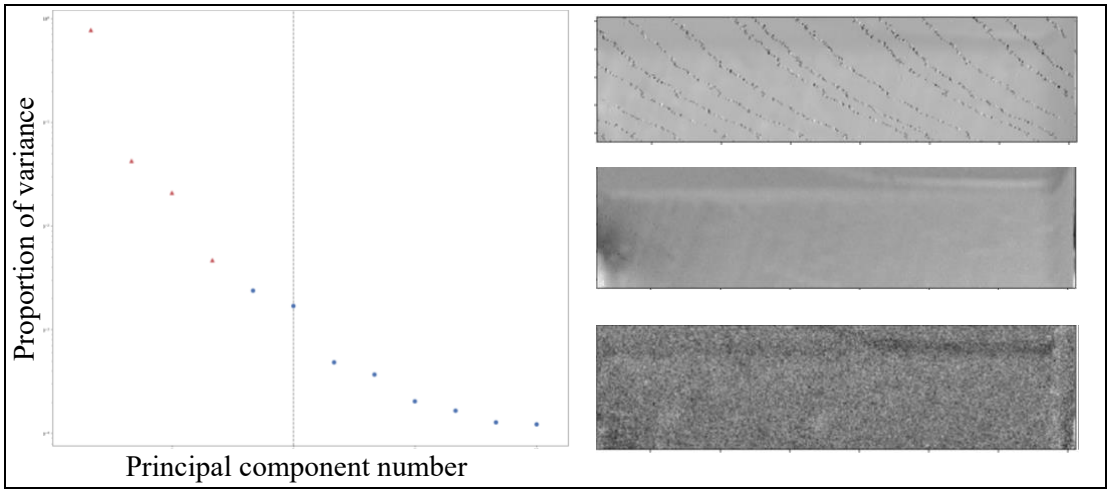

Figure 5. PCA scree plot with 12 components and 1st, 6th and 12th (from top down) components shown individually

Principal component analysis is performed on the aligned data set to determine the number of variance components to pass through the NMF algorithm. By inspecting the scree plot an estimate of the number of significant components to keep can be determined. This is displayed by a vertical dashed line set at around 0.01-0.005 of the proportion of variance, which is determined by a user defined limit. This is a small component of the total data but it is possible that concentrated areas of isolated copper atoms may be excluded if too few components are selected. The first principal component contains a proportion of around 0.8 (or 80%) of the total variance (data set) with the second principal component around 0.1 or 10%. The scree plot alone is often not enough to determine a suitable number of components to keep, so the individual PCA components can be viewed. Looking at the initial components it is clear that even the 6th component contains useful data and it is not until the 12th component that the signal is becoming mostly noise. To ensure only noise is excluded 20 components are passed through the NMF algorithm.

3.5. Non-negative matrix factorisation (NMF)

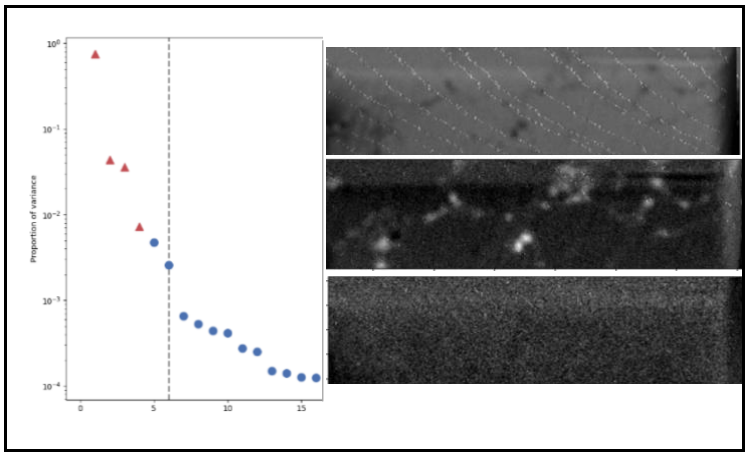

Figure 6. NMF scree plot and resulting 1st, 6th and 9th (top to bottom) variance components plotted individually

After performing NMF it is possible to check whether all of the components which have been passed through the algorithm are needed. Viewing the scree plot (Fig 6) shows a much more varied result and by the 13th principal component the proportion of variance is almost down at 0.0001. This is much faster than the original PCA and confirms that the first 20 components are more than enough to keep and retain the maximum proportion of the signal. The individual components can be viewed once again (Fig 6) to ensure that there is no important information being discarded. Reconstructing the EDS spectrum with the first 20 components gives a much cleaner noise reduced spectrum (Fig 4b) that will make quantification results much more reliable. Each individual peak can clearly be seen and the addition of a background spectrum will therefore be much easier, ensuring that any smaller elemental peaks are not removed. The machine learning algorithm was successful in its purpose in removing noise to produce a smoother and more easily analysable spectrum.

3.6. Background Windows (BW) and Integration Windows (IW)

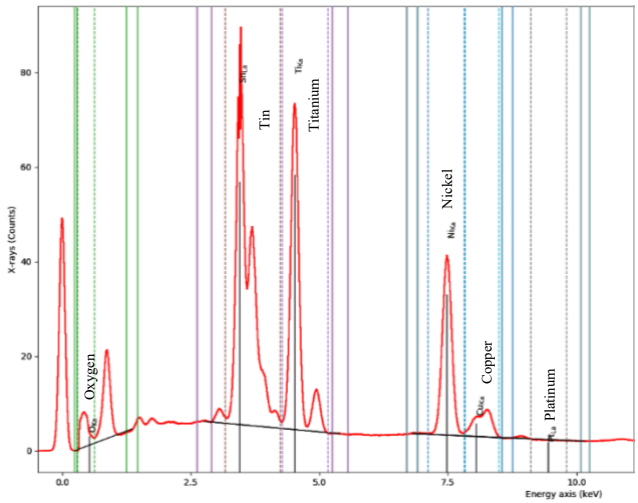

Figure 7. EDS spectrum with background (solid line) and integration (dotted line) windows

Background window and integration windows are at first randomly set to take an initial rough measurement. These can be amended later so that they accurately encompass all of the peaks relating to the desired element. Having the correct background windows is important to ensure an accurate removal of the background spectrum. If a background window encompasses a small peak this can distort the values and potentially remove vital data. In Figure 7, the horizontal black lines indicate what will be removed below the combined spectra (red line) when calculating intensities. It was seen that it follows the predicted Bremsstrahlung correlation and it does not cut off any useful peaks, so is a good selection for this specific data set.

To determine which integration windows to pick, Hyperspy has a method for displaying the energies at which peaks are expected with the majority of the peaks lining up with their respective lines. There are some peaks that do not correspond to a line so to determine whether we need to include these in the integration windows another method must be used. This can involve searching the corresponding energy spectra for the elements and seeing if there is a split peak for the elements tin and titanium. If there is access to a Bruker Espirit software package the data can be imported into this and each peak can be quickly identified. From this analysis each of the lower peaks at higher energies for tin and titanium were found to be relating to these elements, so were included in the integration windows. The peak around 1keV above the oxygen line was determined to most likely correspond to an aluminium emission line, so it is likely that a component of the detector (made of aluminium) has caused this spike. The

spike is also not completely constant throughout and since it does not correspond to an oxygen oxide emission it is not included in this integration window. At the copper emission line there is not one definite peak and the spectra appears to be a combination of two peaks. Using Bruker, it suggests the left side of this combined peak is a contribution from the copper emission line and the right peak is a contribution from a nickel emission line. There are multiple ways to try and handle this data, either selecting the nickel integration window to include the whole of the smaller peak or attempt to split the peak in half. However, many counts for both will be lost if we do this as this package cannot determine which corresponds to which emission. As the main focus of this application is to prove the successfulness of an alignment and noise reduction algorithm and not a final composition, the smaller peak was left to represent the copper emission only. This will lead to a slightly higher total percentage of copper and lower percentage of nickel in the final quantification. The peak at 0 keV is caused by the noise of electronics in the detector and can be ignored completely.

3.7. EDS quantification (intensities and percentages)

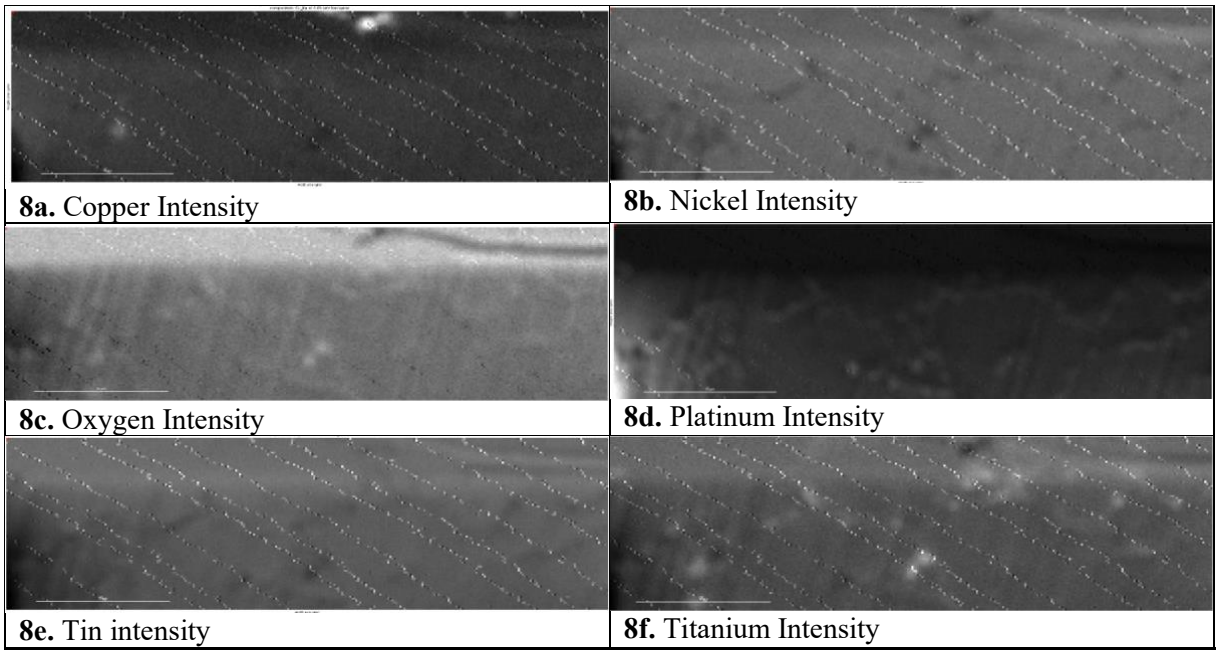

8a. Copper Intensity | **8b.** Nickel Intensity

8c. Oxygen Intensity | **8d.** Platinum Intensity

8e. Tin intensity | **8f.** Titanium Intensity

Figure 8. Intensity spectrum for 6 elements with x and y axis the dimensions of the sample and the individual pixel brightness displaying the intensity (note: brighter pixels indicate a higher intensity)

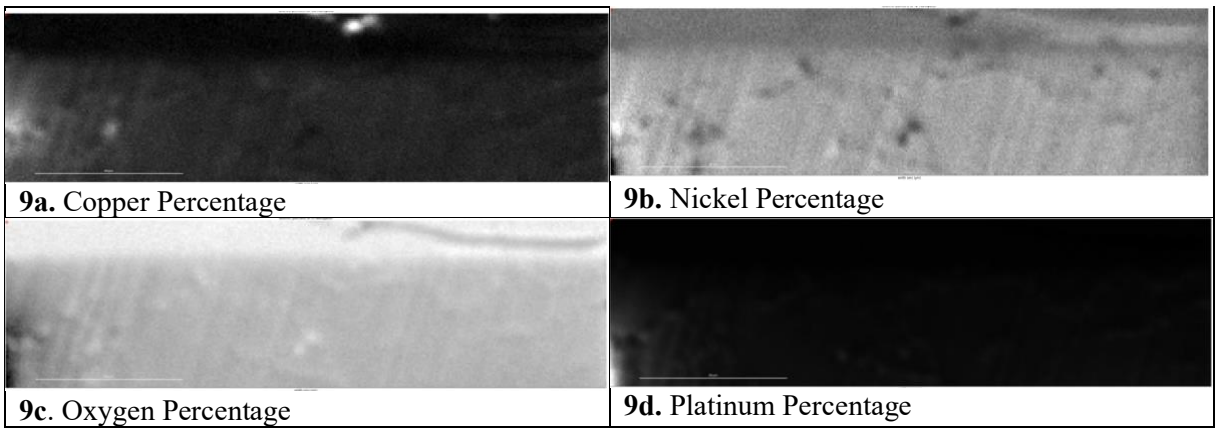

9a. Copper Percentage | **9b.** Nickel Percentage

9c. Oxygen Percentage | **9d.** Platinum Percentage

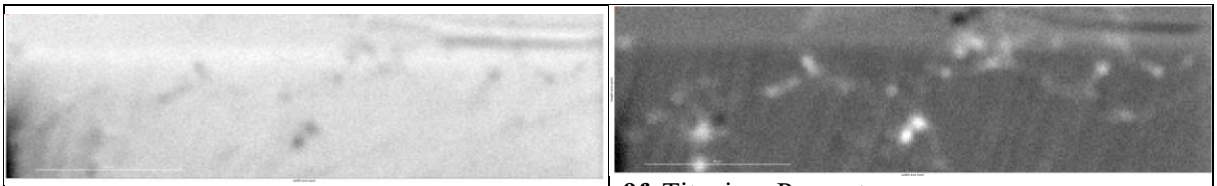

9e. Tin Percentage | **9f.** Titanium Percentage

Figure 9. Atomic percentages of elements with x and y axis the dimensions of the sample and the individual pixel brightness displaying the percentage (note: brighter pixels indicate a higher percentage)

For final quantification for analysis of a single slice the figures viewed contain the end faces and a section of the main body of the sample which is not changed between measurements. This allows for analysis of a larger section of the sample and comparison of the effects of milling on the surface measurements of the sample. Intensity maps (Fig 8) give the overall peak intensity found in each pixel for each corresponding element. These can give an idea of the distribution of elements in the sample whilst retaining more of the overall structure, compared to an atomic percentage map which is better for displaying the overall composition and what elements are more prevalent. The periodic stripes of white spots of increased counts arise from timing errors in the EDS acquisition spectra and can be ignored. When producing a thermoelectric metal-alloy the 3 core metals (Sn, Ti, Ni) are mixed with a small amount of copper to improve electrical conductivity. The aim is to mix all 4 metals equally throughout the crystal but often metals concentrate to form areas of high density of one specific metal. This is most common with copper and from Figure 9a it can be seen that there is a clear section of high intensity of copper line emissions and equally there is a deficiency in the other core elements (b, e, f).

Mixing of metals to form a crystal results in different alloy phases where the composition of each individual metal differs in separate sections of the sample. titanium shows multiple areas of higher intensity which correspond to low intensities in nickel and tin but a high intensity for oxygen emission. This suggests that these areas are in fact titanium oxides and one bright section in the lower central region of Figure 9f indicates there is composition of 32% titanium, 1.5% metal oxide, 19% nickel and 37% tin. There is further evidence of potential other oxides in figures 9c and 10c, where it shows a higher percentage of oxygen in the upper section of the alloy and a deficiency in nickel but a slight increase in titanium and tin suggesting oxides of both elements are present here. This could be due to the way that the surface was polished, but it is a much more consistent overall distribution. Figures 9 (b, e and f) show a major difference in alloy compositions with the upper section as discussed shows a composition of 23% nickel, 22% titanium, 48% tin and 3% metal oxide (oxygen) while the lower section shows an alternative composition of 27% nickel, 18% titanium, 46% Tin and 1% metal oxide. This separation of upper and lower corresponds to the milled top section and un-milled lower section and suggests that the act of exposing the sample to the air increases the number of oxides produced. Throughout the rest of the sample there are a large number of smaller separate phases making the total sum difficult to count accurately. For platinum there is only a small section of high intensity (Fig. 8d and 9d). This is in the bottom left corner and corresponds to a lower intensity in all other elemental maps giving a maximum percentage of 75%. This is most likely from a platinum holder that is at the side of the sample and remains constant between slices confirming this suspicion.

Table 2. Comparison of alloy compositions

Element	**Hyperspy***	**Bruker**	**Difference**
Copper	5%	2.4%	2.6%
Nickel	25%	26.7%	1.7%
Oxygen	2%	0%	2%
Platinum	>1%	0.8%	0.2%
Tin	47%	47.7%	0.7%
Titanium	20%	22.3%	2.3%

*Average value from two main alloy phase compositions

From information known about the construction of the sample it was suspected that this metal alloy was approximately 1/3 for each of the core elements tin, nickel and titanium with roughly 1-2% copper doping. From the percentage figures (Fig 9) it was expected that Figures 9b, 9e and 9f would be similar in distribution with the chance of some clustered areas of higher density of a single element. However, from a quick inspection it is clear that there is a much higher percentage of tin present in the sample with the lowest component being titanium. A comparison of the Hyperspy algorithm calculated values against Bruker calculated values confirms what was viewed from inspection. Hyperspy values are given as an average of the two main alloy phases as the Bruker software is not able to differentiate between the top milled section and the lower un-milled and both phases combine to make up the majority of the sample and so together are a good estimate of the total composition.

Hyperspy measures a composition that includes 5% copper which is 2.6% higher than Bruker, but as explained the copper emission peak for Hyperspy includes a contribution from a nickel emission which will account for the large difference in the values. Similarly, nickel shows a 1.7% lower composition in Hyperspy as this secondary peak is missing and if this had been included a closer value would have been determined. The Bruker software does not find any oxygen emission for metal oxides and gave a 0% contribution, this is either a limitation of the Bruker software's quantification or customisation, but in this case the Hyperspy algorithm gave a more detailed overall solution. Platinum constitutes a low overall percentage which is below 1% for Hyperspy since its only contribution comes from the holder and Bruker similarly calculates this at 0.8%. Tin emissions were also found to be much higher than initially expected and including the second tin peak was proved to be the correct decision, as the difference in atomic percentage was 0.7%. Titanium was similarly close to the Bruker calculation, resulting in a difference of 2.3% which is likely accounted for by some oxides that Bruker did not include.

3.8 3D Visualisation

Displaying the top milled section alone allowed interactive visualisation of the whole stack and a better understanding of the overall composition of the sample (Fig 10). The end sections in figure 10 of the complete stack are bright suggesting a high copper content. However, this is displaying a section that retained some areas which had no sample information but just noise, so it is just displaying a false copper intensity signal. The real copper signal can be seen throughout the rest of the alloy in the section enclosed by a red circle which shows a high intensity copper region that is present throughout almost the entire width of the sample. A second region (yellow circle) shows more high intensity regions that are located in the centre of the length of the sample, but these have only formed over a few slices or few 10's of slices. Throughout the remainder of the sample there is a consistent scattered intensity signifying the 2-3% copper content that has been doped in this sample.

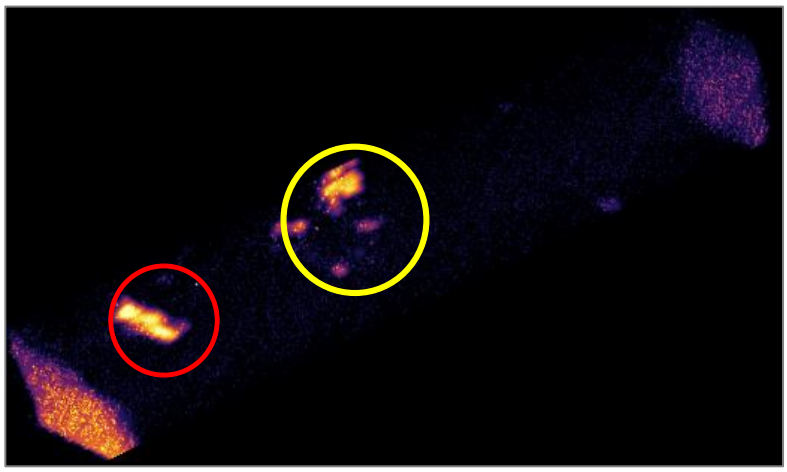

Figure 10. 3D reconstruction of the sample showing only copper

3.9. Sources of Error

Error is a vital component for all experimental work and must be taken into consideration even if it is not possible to determine an absolute value for the error. In this experiment there are sources of error it would be possible to determine a value for, and others that it would not. When measuring the data the electron microscope has errors associated with its use that limit its accuracy of measurements.

The alignment algorithm has an error in the values it determines for the final shift vectors, but it is difficult to determine a value as running the algorithm on the same area multiple times does not give the exact same values. A value for error could be determined by running the same data set multiple times and taking an average of the shifts for the shifts to use and the maximum changes in the shifts up and down as the error boundaries. The shift values determined by the algorithm give shifts that are not just pixel values but when performing shifts on the EDS data. This can only be done by pixel shifts and so shift vectors have to be rounded increasing the error boundaries in these measurements. For non-negative matrix factorisation, matrix A is split into multiple matrices (B,C) that multiply to roughly form the original matrix A, the error in this is found from Error = |A – BC|, which is the difference between the original matrix and the recombination matrix BC.

Further uncertainty can arise from measurements of peak intensity as regions are selected by sight and it is possible to miss counts which may lead to a wrong overall percentage or error in the true percentage. Estimated windows are set by distances either side of the full width half maximum (the distance between two points on either side of a peak which are at half the maximum height of the peak) but it was found that these did not encompass the full emission peak so there is no implemented computation method to ensure that all of the spectra are measured. The cliff-lorimer quantification method will also have errors that have been propagated from the intensity and errors in the k-factors that will contribute to an overall error in the atomic percentages.

When taking measurements with the electron microscope there is the possibility that electrons can scatter off of materials not present in the sample or components of the microscope producing unexpected spectra in sections of the sample that you would have not expected. In the experiment this occurred where an aluminium emission peak was observed suggesting that a section of the microscope was made of aluminium. For aluminium it is not a major problem as it does not cover any spectra that are being measured. However, if it had been one of the elements in the sample or an emission line close by this could have skewed the data. Changes in air pressure or temperature over the course of a measurement can lead to fluctuations along with vibrations moving the sample leading to drift. For the electron microscope used, much better results were gained when the nearby subway was not in use. Furthermore, improper preparation of the sample, either poor polishing or low electrical conductivity can lead to low counts and make it harder to determine results.

In the data used the electron microscope recorded an intensely bright pixel at regular occurrences throughout the sample and can be seen as diagonal lines going downwards from left to right in most of the intensity plots (Fig 8). This result is not seen to be translated into the percentage results as this quantification method uses ratios of peaks, and so any pixel where all of the intensities have been artificially increased the ratio will still remain the same.

4. Conclusion

An algorithm able to align, reduce noise and quantify to a good level of accuracy of a set of SEM and EDS data has been achieved. The need for alignment was seen visually and the results of alignment could also be viewed to have been successful. The algorithm allowed for more user input and adjustment than the typical Bruker software and the final results compared well with those found using the Bruker methods, even proving to have some quantification advantages over this method as it was able to detect metal oxides. The observation of intensity and atomic percentage plots showed the wide variation in alloy phases which would be clearer if viewing the EBSD data. The quantification values for atomic percentage agreed to less than 3% for all elements with reasons for the differences due to sources of error and alternative ways of quantification for elemental peaks.

References

[1] A comprehensive review of thermoelectric technology: Materials, applications, modelling and performance improvement. S Twaha, J Zhu, Y Yan and B Li. Renewable and Sustainable Energy Reviews Vol. 65, 698-726 (2016)

[2] Is Scanning Electron Microscopy/Energy Dispersive X-ray Spectrometry (SEM/EDS) Quantitative?; D Newbury and N Ritchie, SCANNING VOL. 35, 141-168 (2013)

[3] Carbon Nanomaterials in Biomedicine and the Environment by Z Mansurov. Pgs 3-11. (2020)

[4] Analytical Transmission Electron Microscopy. W Sigle, Annual Review of Materials Research 35:1, 239-314 (2005)

[5] Charging effects in the scanning electron microscope, T Shaffner and R Van Veld, Journal of Physics E Scientific Instruments 4(9):633 (2001)

[6] https://hyperspy.org, Hyperspy: multi-dimensional data analysis toolbox, F de la Pena et al (2019)

[7] Automated spatial drift correction for EFTEM image series; B Shaffer, W Grogger and Gerald Kothleitner; Ultramicroscopy, Vol 102 Issue 2, pgs 27-36 (2004)

[8] Effect of Shot Noise and Secondary Emission Noise in Scanning Electron Microscope Images. K S Sim, J T L Thong and J C H Phang: SCANNING VOL. 26, 36-40 (2004)

[9] Principal Component Analysis. J Lever et al, Nature Methods 14, 641-642 (2017)

[10] Three-dimensional imaging of localised surface plasmon resonances of metal nanoparticles. O Nicoletti, F. de la Pena, R Leary, D Holland, C Ducati and P Midgley, Nature **502**, 80-84 (2013)

[11] The quantative analysis of thin specimen. G Cliff and G W Lorimer. Journal of Microscopy **103**, 203-207 (1975)

[12] Recent advances in thermoelectric performance of half-heusler compound. S Poon, Metals – Open access Metallurgy Journal 8(12):989 (2018)

[13] Electronic and thermoelectric properties of half-heusler alloys. G Poon, Semiconductors and Semimetals vol 70, 37-75 (2001)

[14] Improved quantification of grain boundary segregation by EDS in a dedicated STEM. U Alber, H Mullejans, M Ruhle, Ultramicroscopy **69**, 105-116 (1997)